ELSEVIER

Physica D 130 (1999) 232–254

PHYSICA D

Travelling waves in chains of pulse-coupled integrate-and-fire oscillators with distributed delays

P.C. Bressloff *, S. Coombes

Nonlinear and Complex Systems Group, Department of Mathematical Sciences, Loughborough University, Loughborough, Leicestershire, LE11 3TU, UK

Communicated by J.P. Keener

Abstract

We analyse travelling waves in a chain of pulse-coupled integrate-and-fire oscillators with nearest-neighbour coupling and delayed interactions. This is achieved by approximating the equations for phase-locking in terms of a singularly perturbed two-point (continuum) boundary value problem. The latter has a solution provided that a self-consistent value for the collective frequency of oscillations can be found. We investigate how the qualitative behaviour of travelling waves depends on the distribution of natural frequencies across the chain and the form of delayed interactions. A linear stability analysis of phase-locked solutions is carried out in terms of perturbations of the firing times of the oscillators. It is shown how travelling waves destabilize when the detuning between oscillators or the strength of the coupling becomes too large. ©1999 Elsevier Science B.V. All rights reserved.

1. Introduction

One of the oldest problems in dynamics is the behaviour of coupled nonlinear oscillators, dating back to Huygen's observations of mutual synchronization of pendulum clocks in the seventeenth century. In more recent times there has been a renewed interest in coupled oscillators stimulated by a diverse range of applications including biological rhythms [1,2], chemical oscillators [3], Josephson junction arrays [4,5] and laser arrays [6,7]. An important theoretical technique for analysing such systems is to work in the weak coupling regime where invariant manifold theory [8] and averaging theory [9] can be used to reduce the dynamics to a set of phase equations in which the relative phase between oscillators is the relevant dynamical variable (see for example, [10–12]). This phase reduction method has been applied to a number of important physical and biological systems. For example, an averaged phase equation has been used to describe a linear series array of overdamped, resistively loaded Josephson junctions [13], and this has elucidated the integrable structure of the system [14]. In the biological context, phase equations have been used to study travelling waves in chains of weakly coupled oscillators that model processes such as the generation

* Corresponding author. E-mail: p.c.bressloff@lboro.ac.uk.

0167-2789/99/$ – see front matter ©1999 Elsevier Science B.V. All rights reserved.
PII: S0167-2789(99)00013-5

and control of rhythmic activity in central pattern generators (CPGs) underlying locomotion [15,16] and peristalsis in vascular and intestinal smooth muscle [11]. Related phase models (see e.g. [17]) have been motivated by the observation that synchronization and waves of excitation can occur during sensory processing in the cortex [18,19].

One of the characteristic features of a variety of biological oscillators is that they communicate with each other by firing sudden pulse-like discharges. Modelling the detailed shape of these pulses requires a system of smooth differential equations with several degrees of freedom for each oscillator. One well known example is the Hodgkin–Huxley model of excitable nerve tissue that describes the generation of an action potential due to the activation–deactivation of a number of voltage-dependent ionic gates [20]. Analysing a network of Hodgkin–Huxley neurons is a difficult task due to the complexity of the single-neuron model. This motivates the application of the phase reduction method (for weak coupling) to reduce the network dynamics to a system of phase equations with the phase interaction function constructed from the single neuron dynamics. The latter has been carried out explicitly for the Hodgkin–Huxley model [21]. An alternative approach is to neglect details concerning the shape of a pulse by considering an *integrate-and-fire* model [22]. The integrate-and-fire model has been used to study flashing fireflies [23], cardiac pacemaker cells [24], and biological neural networks [25–30]. Mutual synchronization of integrate-and-fire oscillators has also recently sparked interest within the physics community due to certain parallels with stick-slip models and self-organized criticality [31].

Although considerable simplification is achieved by working with integrate-and-fire oscillators, the mathematical analysis is still a challenging problem since the state of the system changes discontinuously at certain discrete time (threshold crossing) events so that a complete description in terms of smooth ordinary differential equations is no longer possible. Significant progress can be made, however, once it is realized that in the case of phase-locked solutions such as synchronous states and travelling waves, the system can be described in terms of a set of phase equations involving the relative shifts in the firing times of the oscillators (with the collective frequency of the oscillators determined self-consistently). These steady-state phase equations have the same formal structure as those obtained using phase reduction methods, with the important additional feature that they are also valid in the strong coupling regime. Thus various analytical techniques developed for studying phase-locking in weakly coupled oscillators may be extended to the case of integrate-and-fire oscillators with arbitrary coupling.

In this paper we present a detailed analysis of phase-locking in networks of integrate-and-fire oscillators. For concreteness, we consider the particular problem of travelling waves along chains of integrate-and-fire oscillators with local, delayed interactions. A corresponding analysis of rings of pulse-coupled oscillators based on group theoretic methods has been presented elsewhere [32,33]. We begin in Section 2 by reviewing relevant results concerning phase-locking and travelling waves in chains of weakly coupled limit cycle oscillators. We then derive conditions for phase-locking in a chain of integrate-and-fire oscillators for arbitrary coupling strength (Section 3). We also derive conditions for the linear stability of phase-locked solutions by considering small perturbations of the firing times. In Section 4 we extend a continuum approximation method introduced by Kopell and Ermentrout [34] to analyse travelling waves in long chains of integrate-and-fire oscillators. Finally, in Section 5 we study through numerical examples how various instabilities arise with changes in the degree of anisotropy, the coupling strength and the distribution of external inputs.

Note that one possible application of our work is to the study of central pattern generators for locomotion. The generation and control of rhythmic activity results from a combination of synaptic interactions, intrinsic membrane properties and network connectivity. Guided by the study of small networks in the spinal cord of the lamprey or Xenopus tadpole and other experimentally accessible systems the fundamental properties of neurons that contribute to rhythm generation are being uncovered. It is likely that each oscillator is actually a local subnetwork of neurons rather than a single endogenous pacemaker cell. Since the precise details underlying such oscillators are still unknown the aim of our mathematical analysis is not to provide an accurate model of CPGs but rather to gain insight into the general forms of behaviour that chains of pulse-coupled oscillators can exhibit.

2. Phase-locking in chains of weakly coupled limit cycle oscillators

In an important series of papers, Ermentrout and Kopell carried out a detailed study of the dynamics of a chain of weakly coupled limit cycle oscillators [11,34,35]. A particular version of the system of equations that they considered is (for anisotropic, nearest neighbour coupling)

$$\dot{X}_n = F(X_n) + \epsilon\left[G^+(X_{n+1}, X_n) + G^-(X_{n-1}, X_n)\right], \tag{1}$$

where $X_n \in R^k, n = 1, \ldots, N+1, F : R^k \to R^k, G^\pm : R^{2k} \to R^k$ and the boundary conditions are $G^+(X_{N+2}, X_{N+1}) \equiv 0 \equiv G^-(X_0, X_1)$. In the absence of any coupling ($\epsilon = 0$), the nth oscillator is assumed to have a stable limit cycle with frequency ω_n. In the case of weak coupling, $\epsilon \ll 1$, it was proven using invariant manifold theory that there exists an asymptotically stable invariant torus of dimension $N+1$. Moreover, phase variables $\theta_n \in R \backslash Z, n = 1, \ldots, N+1$, may be chosen so that the dynamics on the torus can be expressed in the form [11]

$$\begin{aligned}
\dot{\theta}_1 &= \omega_1 + \epsilon h^+(\theta_1, \theta_2, \epsilon);\\
\dot{\theta}_n &= \omega_n + \epsilon[h^+(\theta_n, \theta_{n+1}, \epsilon) + h^-(\theta_n, \theta_{n-1}, \epsilon)];\\
\dot{\theta}_{N+1} &= \omega_{N+1} + \epsilon h^-(\theta_{N+1}, \theta_N, \epsilon);
\end{aligned} \tag{2}$$

where $h^\pm$ is a periodic function of its 2π arguments that depends on the nature of the coupling and on the dynamics in a neighbourhood of a limit cycle. If $\omega_n = \omega_1 + O(\epsilon)$ then averaging theory [9] implies that

$$\begin{aligned}
\dot{\theta}_1 &= \omega_1 + H^+(\theta_2 - \theta_1) + O(\epsilon^2);\\
\dot{\theta}_n &= \omega_n + [H^+(\theta_{n+1} - \theta_n) + H^-(\theta_{n-1} - \theta_n)] + O(\epsilon^2);\\
\dot{\theta}_{N+1} &= \omega_{N+1} + H^-(\theta_N - \theta_{N+1}) + O(\epsilon^2);
\end{aligned} \tag{3}$$

with

$$H^\pm(\phi) = \int_0^{2\pi} h^\pm(\tau, \tau + \phi)\, d\tau. \tag{4}$$

A basic issue concerning the dynamics of a chain of coupled oscillators is the conditions under which phase-locking can occur, by which we mean a stable periodic solution to Eq. (3) and hence to Eq. (1). Such a solution takes the form $\theta_n(t) = \Omega t + \phi_n$, where Ω is the collective frequency of oscillations and the ϕ_n's are constant. Of particular interest from the viewpoint of biological systems are travelling wave solutions for which the phase ϕ_n varies monotonically along the chain (see e.g. [15]). For sufficiently small ϵ, phase-locked solutions of Eq. (3) correspond to fixed points of an associated system of equations for the phase-differences $\psi_n = \phi_{n+1} - \phi_n, n = 1, \ldots, N$:

$$\dot{\psi}_n = \Delta_n + H^+(\psi_{n+1}) - H^+(\psi_n) + H^-(-\psi_n) - H^-(-\psi_{n-1}) \tag{5}$$

with boundary conditions

$$H^-(-\psi_0) \equiv 0 \equiv H^+(\psi_{N+1}); \tag{6}$$

where $\Delta_n = \omega_{n+1} - \omega_n$ and the time t has been rescaled according to $t \to \epsilon t$. Note that fixed points of Eq. (5) are independent of the collective frequency Ω; the latter is determined from the equation

$$\Omega = \omega_1 + H^+(\psi_1) + O(\epsilon^2). \tag{7}$$

One finds that there are at least two different mechanisms that can generate travelling wave solutions. The first is based on the presence of a gradient of frequencies along the chain, that is, 1_n has the same sign for all n, with the wave propagating from the high frequency region to the low frequency region. This can be established explicitly in the case of an isotropic, odd interaction function, $H^{\pm}(\phi) = H(\phi) = -H(-\phi)$. Eq. (5) then simplifies according to

$$\dot{\theta}_n = 1_n + H(\theta_{n+1} - \theta_n) + H(\theta_{n-1} - \theta_n) \tag{8}$$

so that fixed point solutions $\theta = (\theta_1, \ldots, \theta_N)$ satisfy the matrix equation

$$\mathbf{H}(\theta) = -\mathbf{A}^{-1}\mathbf{D}, \tag{9}$$

where $\mathbf{H}(\theta) = (H(\theta_1), \ldots, H(\theta_N))^{\mathrm{T}}$, $\mathbf{D} = (1_1, \ldots, 1_N)^{\mathrm{T}}$, and $\mathbf{A}$ is a tridiagonal matrix with components $A_{ii} = -2$, $A_{i,i+1} = A_{i+1,i} = 1$. For the sake of illustration suppose that $H(\phi) = \sin 2\pi\phi$. Then a solution θ will exist if every component of $\mathbf{A}^{-1}\mathbf{D}$ lies between ± 1. Let $a_0 = \max_n\{|(\mathbf{A}^{-1}\mathbf{D})_n|\}$. If $a_0 < 1$ then for each $n = 1, \ldots, N$ there are two distinct solutions $\theta_n^{\pm}$ in the interval [0,1] with $H'(\theta_n^-) > 0$ and $H'(\theta_n^+) < 0$. In other words, there are 2^N phase-locked solutions. Linearizing Eq. (8) about a phase-locked solution θ and exploiting the structure of the matrix $\mathbf{A}$, it can be proven that only the solution $\theta^- = (\theta_1^-, \ldots, \theta_N^-)$ is stable. Assuming that the frequency gradient is monotonic, this solution corresponds to a stable travelling wave. When the gradient becomes too steep to allow phase-locking (i.e. $a_0 > 1$), two or more pools of oscillators (frequency plateaus) tend to form that oscillate at different frequencies [11].

Waves induced by frequency differences are important in peristalsis [36,11] and are also known to exist in certain central pattern generators (CPGs) for swimming including the leech [37] and the Xenopus tadpole [38]. However, there is no evidence for frequency gradients in the lamprey CPG [15]. Moreover, in contrast to the waves observed in the lamprey CPG, waves produced by a frequency gradient do not have a constant speed or, equivalently, constant phase lags along the chain. Constant speed waves in a chain of identical oscillators can be generated by an alternative mechanism based on properties of the coupling. This can be understood by considering a chain of identical oscillators with one-way coupling. Setting $H^- = 0$ and $1_n = 0$ in Eq. (5) shows that if there exists a non-zero value $\bar{\ }$ at which $H^+(\bar{\ }) = 0$; $H^{+\prime}(\bar{\ }) > 0$ then there exists a stable travelling wave solution with constant phase lag, $\theta_n = \bar{\ }$ for all n. An interaction function having the above so-called *edge property* occurs for almost all kinds of coupling including chemical synapses. One important exception is that of electrical synapses (gap junctions) where the coupling is diffusive so that $G^{\pm}(U, U) = 0$ in Eq. (1) and the hence $H^{\pm}(0) = 0$. If the coupling is in both directions, as in the lamprey CPG, then the analysis is considerably more involved. Nevertheless, it can be shown that for non-diffusive, anisotropic coupling, $H^+ \neq H^-$; $H^{\pm}(0) \neq 0$, and sufficiently long chains of identical oscillators, there exist stable travelling waves with constant phase lags (except in a small boundary layer). The method of proof involves a continuum limit analysis in which solutions of Eq. (5) are shown to converge to solutions of a class of nonlinear, singularly perturbed, two-point boundary value problems [34,35].

An important question concerning the dynamics of weakly coupled oscillators is how large the coupling strength is permitted to be without the loss of the invariant torus. If the rate of attraction to the limit cycle is sufficiently strong an equation of the form (2) also holds in the strong coupling regime. One then has a phase model whose interaction functions no longer depend on phase differences (since averaging theory is no longer appropriate). Such a model can exhibit more complex behaviour than the averaged model. In particular, for sufficiently large interactions, the coupling can act to stop all oscillations leading to so-called *oscillator death*. This has been studied in some detail for several models of excitable cells in which the function $h^{\pm}$ naturally takes the product form [39,40]

$$h(\theta_n, \theta_m) = R(\theta_n)P(\theta_m), \tag{10}$$

where $P(\cdot)$ is a positive pulse-like function (associated with conductances) and $R(\cdot)$ is analogous to the phase-response curve for a forced oscillator [2].

In this paper, we shall consider another class of models for coupled excitable cells that is based on the integrate-and-fire model of neural oscillators. Such a model, which may be regarded as a reduction of the Hodgkin–Huxley model [41], preserves the pulse-like nature of neural interactions without being concerned about the particular details of the shape of action potentials. It will allow us to incorporate various details concerning neural interactions, such as axonal transmission delays and synaptic processing, in a relatively straightforward manner. As we shall establish in Section 3, one of the interesting features of integrate-and-fire chains is that the conditions for phase-locking are formally identical to those derived from Eq. (3) except that the former hold for all values of the coupling strength rather than just in the weak coupling limit. Thus one can extend the continuum approximation method of Kopell and Ermentrout [34] to analyse travelling waves in chains of integrate-and-fire oscillators, with the important additional features that the analysis holds for arbitrary values of the coupling strength (see Section 4).

3. Phase-locking in chains of integrate-and-fire oscillators

3.1. The model

Consider a chain of $N+1$ integrate-and-fire oscillators labelled $n = 1, \ldots, N+1$. Let $U_n(t)$ denote the state of the nth oscillator at time t. Suppose that the variables $U_n(t)$ satisfy the set of coupled equations

$$\dot{U}_n(t) = -\frac{U_n(t)}{\tau_s} + I_n + \sum_{\langle m,n\rangle} \hat{E}_m(t) \tag{11}$$

for $0 < U_n < 1$ where $\langle \cdot, n\rangle$ denotes summation over nearest neighbours of n. Here τ_s represents a membrane time constant and g corresponds to a conductance (in appropriate units). For convenience, we fix the units of time by setting $\tau_s = 1$. Typical values of the membrane time constant are 5–20 ms. Eq. (11) is supplemented by the condition that the oscillator fires a single pulse or spike whenever $U_n = 1$ and that the state is immediately reset to $U_n = 0$. In Eq. (11), I_n denotes a fixed external input and $\hat{E}_n$; $n = 1, \ldots, N+1$, represents the input from the nth oscillator. We shall assume that $I_n > 1$ so that in the absence of any coupling ($g = 0$) each oscillator fires at a rate $1/\bar{T}_n$ with $\bar{T}_n = \ln[I_n/(I_n - 1)]$. The inputs take the form

$$\hat{E}_m(t) = \int_0^\infty \eta(\tau) E_m(t-\tau)\, d\tau \tag{12}$$

for $m = 1, \ldots, N+1$, where $E_m(t)$ is the sequence of spikes transmitted from the mth oscillator at time t and $\eta(\tau)$ specifies a distribution of delayed connections. Neglecting the shape of an individual pulse, each spike train can be represented as a sequence of Dirac delta-functions

$$E_n(t) = \sum_{j=-\infty}^{\infty} \delta(t - T_j^n); \tag{13}$$

where T_j^n is the jth firing-time of the nth oscillator, that is, $U_n(T_j^n) = 1$.

We decompose $\eta(\tau)$ as $\eta(\tau) = \eta_e(\tau) - \eta_i(\tau)$ where $\eta_{e,i}(\tau)$ represent distributions of excitatory (e) and inhibitory (i) connections between neighbouring oscillators with $\eta_{e,i}(\tau) \geq 0$ for all τ and $\int_0^\infty \eta_{e,i}(\tau)\, d\tau = W_{e,i} < \infty$. In neural circuits underlying locomotion [38] and cortical microcircuits [42], there is a mixture of excitation and inhibition mediated through synaptic interactions. In fact both inhibitory and excitatory post synaptic potentials (PSPs) have

some finite rise and fall time. Moreover, the former are often generated by inhibitory interneurons leading to another form of delay in interaction process. Motivated by such architectures we take

$$\alpha_e(t) = \frac{t}{\tau^2}\exp(-t/\tau)H(t); \qquad \alpha_i(t) = \alpha_e(t-\tau_d)H(t-\tau_d); \tag{14}$$

where $H(x) = 1$ if $x \geq 0$ and $H(x) = 0$ if $x < 0$. In this case the inhibitory pathway is delayed with respect to the excitatory one and both forms of PSP are assumed to be identical with $W_{e;i} = 1$. An analogous construction is considered by Ritz et al. [43]. For the moment we shall also assume that the connections between oscillators are isotropic. In Section 4 we shall relax this assumption to allow for anisotropy. This requires the introduction of a pair of distributions for right-directed delayed interactions, $\rho^+(t)$, and similarly for left-directed connections, $\rho^-(t)$.

3.2. Phase-reduction and averaging in the weak coupling limit

We shall first show how in the weak coupling limit Eq. (11) with reset can be reduced to a phase equation of the form (2). Following van Vreeswijk et al. [44], we introduce the phase variable $\theta_n(t)$ according to

$$\Theta(\bmod 1)\ \theta_n(t) + \frac{t}{\bar{T}_n} = \vartheta_n(U_n(t)); \tag{15}$$

where

$$\vartheta_n(U) = \frac{1}{\bar{T}_n}\int_0^U \frac{dx}{I_n - x} = \frac{1}{\bar{T}_n}\ln\left(\frac{I_n}{I_n - U}\right); \tag{16}$$

Under such a transformation Eq. (11) becomes

$$\dot{\theta}_n(t) = R_{\bar{T}_n}(\theta_n(t)) + \frac{t}{\bar{T}_n}\sum_{\langle m;n\rangle}\hat{E}_m(t) \tag{17}$$

with

$$R_T(t) = \frac{1 - e^{-T}}{T}e^t \tag{18}$$

for $0 \leq t < 1$ and $R_T(t+j) = R_T(t)$ for all $j \in \mathbb{Z}$. In the absence of any coupling the phase variable $\theta_n(t)$ is constant in time and all oscillators fire with their natural periods $\bar{T}_n$. For weak coupling, each oscillator still approximately fires at the unperturbed rate but now the phases slowly drift according to Eq. (17). Since the distribution $\rho(t)$ is normalizable with $\rho(t) \to 0$ as $t \to \infty$, we can neglect the contribution to $\hat{E}_m(t)$ from spikes fired sufficiently far in the past. Hence, to first order in ε, we can take the firing-times to be $T_j^n = (j - \theta_n(t))\bar{T}_n$. Under this approximation, Eqs. (12) and (17) lead to the following equation for the shifted phases $\phi_n(t) = \theta_n(t) + t/\bar{T}_n$:

$$\dot{\phi}_n = \frac{1}{\bar{T}_n} + \sum_{\langle m;n\rangle} R_{\bar{T}_n}(\phi_n)P_{\bar{T}_m}(\phi_m) + O(\varepsilon^2); \tag{19}$$

where

$$P_T(t) = \sum_{j=0}^{\infty}\alpha(t+j)/T \tag{20}$$

for $0 \leq t < 1$ and P_T is extended outside this range by taking it to be a periodic function of t.

Comparison of Eq. (19) with Eqs. (2) and (10) shows that R_T may be interpreted as the phase-response curve (PRC) of an individual integrate-and-fire oscillator and P_T is the corresponding pulse-like function that contains all

details concerning the distribution of delays. As discussed in some detail by Hansel et al. (1995), integrate-and-fire oscillators have a type I PRC, which means that an instantaneous excitatory stimulus always advances its phase ($R_T(\phi)$ is positive for all ϕ). On the other hand, in certain cases, limit cycle oscillators based on Hodgkin–Huxley-like models of excitable cells are of type II. That is, an excitatory impulse can either advance or retard the phase depending upon the point on the cycle at which the stimulus is applied ($R_T(\phi)$ takes on both positive and negative values over the domain $\phi \in [0,1]$). Since Eq. (19) was derived in the weak coupling regime, we can simplify it further by assuming that $I_n = I + O(\epsilon)$ and averaging over the period $\bar{T} = \ln[I/(I-1)]$. This leads to an equation of the form (3) with isotropic coupling,

$$\dot{\phi}_n = \omega_n + \sum_{\langle m;n\rangle} H_{\bar{T}}(\phi_m - \phi_n) + O(\epsilon^2) \tag{21}$$

with

$$\omega_n = \frac{1}{\bar{T}_n}$$

and

$$H_T(\phi) = \int_0^1 R_T(\theta) P_T(\theta + \phi)\, d\theta. \tag{22}$$

(Note that an averaged interaction function for integrate-and-fire models was previously computed by Ermentrout [45].) We conclude that in the weak coupling regime, phase-locking can be analysed along the lines described in Section 2 for the given interaction function (22).

A number of points are in order. First, the interaction function $H_{\bar{T}}$ in Eq. (22) depends explicitly on the natural frequency $1/\bar{T}$ of the oscillators. In general, this would mean that the phase-lag induced along a chain by a travelling wave would vary with the speed of locomotion (see Section 2). However, it appears that in certain vertebrates such as the lamprey, the phase-lag is approximately independent of the speed of swimming. Indeed, it is found that the wavelength of a travelling wave is comparable to the length of the animal's body. A possible mechanism for this, based on additional long-range coupling, has been considered by Ermentrout and Kopell [46]. Second, since integrate-and-fire oscillators are of type I the interaction function $H_T(\phi)$ would be positive for all ϕ in the case of purely excitatory interactions. In order to allow for the more general type II form of interaction function, we have assumed that there exists a combination of excitatory and inhibitory interactions between the integrate-and-fire oscillators, see Eq. (14). In particular, $P_T(\phi) = P_T^e(\phi) - P_T^i(\phi)$ where $P_T^{e;i} = \sum_{j=0}^{\infty} \epsilon_{e;i}^{\,j} P_T^{e;i}(\phi + j/T)$. The summation over j is easily performed for $\epsilon_{e;i}$ satisfying Eq. (14) and gives

$$P_T^e(\phi) = \frac{\epsilon^2 e^{-\phi T}}{1-e^{-T}}\left(T + \frac{T e^{-T}}{1-e^{-T}}\right); \qquad 0 \le \epsilon < 1; \qquad P_T^i = P_T^e - \frac{d}{T}. \tag{23}$$

As before, these functions are extended outside their ranges by taking them to be periodic functions of ϕ. For an appropriate combination of excitatory and inhibitory connections it is possible for the effective interaction function of an integrate-and-fire oscillator to be approximately sinusoidal (see Fig. 1).

3.3. Phase-locked solutions for arbitrary coupling

It is possible to study phase-locked solutions of Eq. (11) without the assumption of weak coupling, as we shall now demonstrate. Suppose that every oscillator fires with the same fixed period T, which is to be determined self-consistently. The state of each oscillator can then be characterized by a constant phase $\phi_n \in \mathbb{R}\backslash\mathbb{Z}$, and the firing

Fig. 1. Isotropic interaction function $H_T(I)$ determined by Eqs. (22) and (23) with $\gamma_d = 10$;

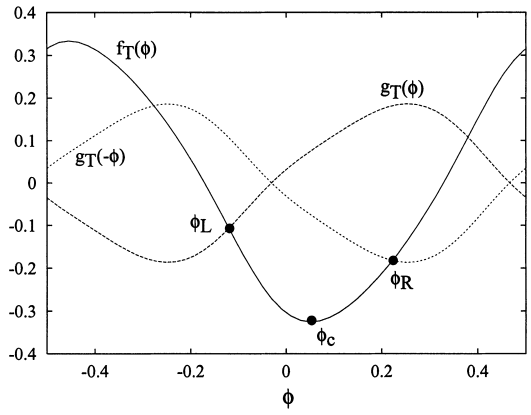

Fig. 7. Functions $f_T(\phi)$, $g_T(\phi)$ for an anisotropic interaction function $K_T^{\pm}(\phi)$ with $\alpha^+ = 5$, $\alpha^- = 10$, $T = 1.2$ and $\gamma_d = 0.6$.

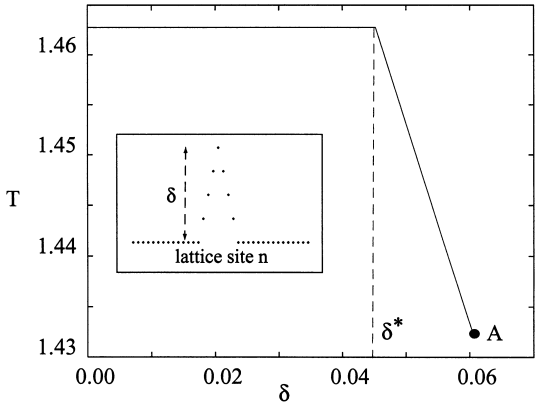

Fig. 8. Self-consistent collective period T for a local perturbation of inputs of size δ and an isotropic interaction function with $\gamma_d = 0.6$, $\alpha = 10$, $\beta = 0.1$ and $\gamma = 0.01$. Results shown are for a chain of 36 integrate-and-fire oscillators. For $\delta < \delta^*$ the collective frequency is determined by $\omega_R(T)$. Beyond δ^* the collective frequency is determined by $\omega_c(T)$. At the point A phase-locking disappears. Inset shows shape of local perturbation of inputs across lattice.

and descending pathways may be incorporated by considering coupling functions that are phase-shifted versions of one another [34].) As an illustration, suppose that we introduce distinct delay parameters $\alpha^+ = 5$, $\alpha^- = 10$ and write $K_T^{\pm}(\phi) = K_T^{\pm}(\phi)$. The resulting functions $f_T(\phi)$ and $g_T(\phi)$ are shown in Fig. 7 where the asymmetry $f_T(\phi_L) \neq f_T(\phi_R)$ is clearly seen. In the case of zero input gradient, this anisotropy will produce a travelling wave down the chain since Q in Eq. (58) will be positive.

5.2. Local regions of non-monotonic input

Assuming that the continuum limit approximation remains valid one may also explore the consequences of non-monotonic distributions for the input $I(x)$. In the uncoupled case, this would induce regions for which there is a local increase or decrease in the natural frequency. We write the input gradient as

$$I(x) = \hat{I}(x) + p(x); \tag{63}$$

where $\hat{I}(x)$ is monotonically increasing in x, say, and $p(x)$ is nonzero only on a finite number of intervals on each of which it has a fixed sign. The parameter δ measures the strength of the local change in input, which we take in numerical experiments to be as shown in the inset of Fig. 8.

Fig. 9. Type I Solution with $_R > \ _c$ determined by $\bullet\ _R.T/$ for a local increase in input at position 20 extending out to neighbours up to three units away is shown with $\diamond$'s and $= \ ^* = 0{:}045$. The type II solution that occurs for a larger $. \ = 0{:}05/$ is shown with $+$'s. In this case the collective frequency is now determined by $\bullet.x\ _c;T/ > \bullet\ _R.T/.$. Results are for an isotropic interaction function with $I_1 = 1{:}3; \ = 0{:}1; \ _d = 0{:}6; \ = 10$ and $= 0{:}01$. Note that the transition region $.n \sim 20/$ is not a layer satisfying the boundary layer equation but is a part of the outer solution.

Fig. 10. Distribution of frequencies T^{-1} across chain for a large local perturbation of inputs of size $= 0{:}1$. All other relevant parameter values are as in Fig. 9.

For the purposes of illustration, suppose that a solution belongs to class (b) of Theorem 2 with $= 0$ and $f''_T > 0$. If is increased but kept sufficiently small such that $\bullet\ _R.T/ > \bullet\ _{max}.T/$ then the solution remains of type I and is different from the $= 0$ solution only on the support of $p.x/$. As increases $\bullet.x\ _c;T/$ grows until $\bullet.x\ _c;T/ = \bullet\ _{max}.T/$. Since $\bullet.x;T/ \ = \hat{I}.x/ + p.x/ \ + 2f\ _T. \ _c/$ and $\hat{I}.x/$ is increasing, $\bullet.x\ _c;T/$ can only exceed $\bullet\ _R.T/$ if is sufficiently large, i.e.

$$> \ ^* \equiv \hat{I}.1/ - \hat{I}.x_c/ + 2f\ _T. \ _R/ - 2f\ _T. \ _c/$$